

ORIGINAL RESEARCH

 OPEN ACCESS

## PD-1 expression conditions T cell avidity within an antigen-specific repertoire

Sylvain Simon<sup>a,b,c</sup>, Virginie Vignard<sup>a,b,c</sup>, Laetitia Florenceau<sup>a,b,c</sup>, B. Dreno<sup>a,b,c</sup>, A. Khammari<sup>a,b,c</sup>, F. Lang<sup>a,b</sup>, and N. Labarriere<sup>a,b,c</sup>

<sup>a</sup>Inserm UMR892/CNRS UMR6299/Univ Nantes, Nantes, France; <sup>b</sup>LabEx IGO "Immunotherapy, Graft, Oncology", Nantes, France; <sup>c</sup>Department of Dermato-cancerology of CHU Nantes, Nantes, France

### ABSTRACT

Despite its negative regulatory role on tumor-specific T cells, Programmed cell death 1 (PD-1) is also a marker of activated tumor-infiltrating T cells. In cancer, PD-1 blockade partially reverses T cell dysfunction allowing the amplification of tumor reactive T cells. Here, we investigated the role of PD-1 signaling on effector/memory human T cells specific for shared melanoma antigens, derived from blood. We documented for the first time the existence of melanoma-specific T cell clones unable to express PD-1. This stable feature was due to the persistent methylation of the *PDCD1* promoter. These PD-1<sup>neg</sup> clones were of lower avidity than their PD-1<sup>pos</sup> counterparts, suggesting that high-affinity-specific T cell clones unable to express PD-1 are not or rarely present in peripheral blood, as they are probably eliminated by negative selection, due to their high reactivity. We also documented the existence of such PD-1<sup>neg</sup> T cell clones in melanoma tumor-infiltrating lymphocytes (TIL), which also exhibited a lower functional avidity than PD-1<sup>pos</sup> TIL clones. This clearly shows that PD-1 expression identifies antigen-specific T cell clonotypes of high functional avidity. Finally, we demonstrated that PD-1 blockade during the *in vitro* selection process of Melan-A-specific T cells favored the amplification of higher avidity T cell clonotypes. This preferential amplification of high-avidity memory T cells upon PD-1 blockade resonates with the expansion of reactive T cells, including neo-antigen-specific T cells observed in anti-PD-1-treated patients. This feature should also be a useful biomarker of clinical efficiency, while providing new insights for adoptive transfer treatments.

**Abbreviations:** PBMC, peripheral blood mononuclear cells; T cell receptor, TCR; TIL, tumor-infiltrating lymphocytes.

### ARTICLE HISTORY

Received 5 September 2015  
Revised 29 September 2015  
Accepted 29 September 2015

### KEYWORDS

Adoptive T cell transfer; immunotherapy; melanoma; Melan-A; PD-1; T cell avidity


### Introduction

PD-1 protein, inducible on many immune cell types,<sup>1,2</sup> is an immunoglobulin superfamily member related to CD28 and is a major T-cell co-inhibitory receptor.<sup>3</sup> The first function assigned to PD-1 was its involvement in immunological peripheral tolerance, maintaining T cell homeostasis by the control of auto-reactive T cells.<sup>4,5</sup> PD-1 has two natural ligands: PD-L1, expressed on activated T cells, monocytes and dendritic cells, and PD-L2, which expression is restricted to dendritic cells and macrophages.<sup>6</sup> Ligation of PD-1 with one of its ligands results in dampening early TCR signaling, through the recruitment of the phosphatases SHP-1 and SHP-2, leading to direct dephosphorylation of signaling intermediates.<sup>3,7</sup> Besides its role in maintenance of physiologic self-tolerance, PD-1 is also implicated in the downregulation of antitumor immunity. Indeed, PD-L1 is commonly expressed on a variety of solid tumors including melanomas<sup>8</sup> contributing to immune escape and is often associated with poor prognosis.<sup>9</sup> Furthermore, melanoma infiltrating lymphocytes are often enriched in PD-1 expressing CD8<sup>+</sup> T cells, which are functionally impaired,<sup>10</sup> but recent studies reported that PD-1, in addition to its

inhibitory functions, could be a useful biomarker to identify tumor-specific T cell repertoire in melanoma.<sup>11</sup> Several clinical trials using blocking anti-PD-1 antibody reported unparalleled effectiveness for cancer immunotherapy, including melanoma, in terms of clinical response rates.<sup>12-14</sup> The search for biomarkers associated with clinical efficiency of PD-1 blockade revealed that both PD-L1 expression on melanoma cells and pre-existing CD8<sup>+</sup> T cell infiltration in the tumor microenvironment should be predictive of clinical response.<sup>15,16</sup> Furthermore, it has been recently described, in a responding NSLCC patient, that anti-PD-1 treatment could induce the proliferation of reactive neo-antigen specific T cells, suggesting that anti-PD-1 therapy can reinvigorate tumor-specific immune response.<sup>17</sup> Obviously, PD-1 blockade has an impact on neo-antigen-specific T cell activation, but its incidence on pre-existing T cells specific for shared tumor antigens remains poorly documented.

Starting from vast T cell repertoires specific for shared melanoma antigens, we sought to decipher the relation between T cell avidity, functional properties, repertoire diversity and PD-1 regulation at the clonal and polyclonal level, for melanoma

**CONTACT** N. Labarriere  [nathalie.labarriere@inserm.fr](mailto:nathalie.labarriere@inserm.fr)

 Supplemental data for this article can be accessed on the publisher's website.

Published with license by Taylor & Francis Group, LLC © Sylvain Simon, Virginie Vignard, Laetitia Florenceau, B. Dreno, A. Khammari, F. Lang, and N. Labarriere  
This is an Open Access article distributed under the terms of the Creative Commons Attribution-Non-Commercial License (<http://creativecommons.org/licenses/by-nc/3.0/>), which permits unrestricted non-commercial use, distribution, and reproduction in any medium, provided the original work is properly cited. The moral rights of the named author(s) have been asserted.

specific effector T cells. We further studied *in vitro* the impact of PD-1 blockade on both diversity and functions of Melan-A-specific T cell repertoire, providing new insights about the role of PD-1 in tumor immunity with strong implications in the field of cancer immunotherapy.

## Results

### PD-1 is differentially expressed on melanoma specific T cells clones

We used the procedure previously described<sup>18</sup> to produce Melan-A<sup>19</sup> and MELOE-1<sup>20</sup> specific T cells from peripheral blood mononuclear cell (PBMC) from an HLA-A2 healthy donor and a melanoma patient. Fig. 1A is a representative

example of the phenotype of specific T cells at different steps of the production process. After the initial peptide stimulation step, lymphocytes enriched in antigen-specific T cells (Fig. 1A, left panel) were sorted and amplified. At the end of the amplification procedure, CD8<sup>+</sup> T cells were fully specific for the cognate antigen (Fig. 1A, middle panel). A fraction of these specific T cells expressed the PD-1 molecule at rest (attested by the absence of CD25 expression), whereas another fraction was PD-1<sup>neg</sup> (Fig. 1A, right panel). In order to explore molecular mechanisms regulating PD-1 expression and to compare the functions of PD-1<sup>neg</sup> and PD-1<sup>pos</sup> T cells, we derived Melan-A and MELOE-1-specific T cell clones by limiting dilution from these polyclonal specific T cells. As illustrated by Fig. 1B, the percentage of PD-1 expression at rest was very variable from one clonotype to another but remained very stable for a given clonotype (repeated measures at rest after seven independent amplification periods). Globally, PD-1<sup>pos</sup> and PD-1<sup>neg</sup> T cell clones exhibited the same phenotype of effector-memory T cells (CD45RO<sup>pos</sup>, CD27<sup>neg</sup>, CD28<sup>low</sup>, CD62-L<sup>low</sup>) and PD-1 expression was not associated with other exhaustion or inhibition markers (CTLA-4<sup>neg</sup>, BTLA<sup>low</sup>, Tim-3<sup>low</sup>, CD95<sup>low</sup>) (Table S1). We thus selected three pairs of PD-1<sup>pos</sup> and PD-1<sup>neg</sup> specific T cell clones, from the same healthy donor or melanoma patient, indicated with arrows on the Fig. 1B. We tested the ability of these T cell clones to express PD-1 when stimulated by various stimuli: specific peptides, anti-CD3 Ab (OKT3), melanoma cell lines expressing Melan-A and MELOE-1 antigens or PMA-CaI. As shown in Fig. 1C, the fraction of PD-1 expressing T cells increased upon stimulation for PD-1<sup>pos</sup> T cell clones (solid lines), regardless of the stimulation mode, whereas PD-1<sup>neg</sup> T cell clones (dotted lines) remained unable or poorly able to express this molecule even when bypassing TCR signaling using PMA-CaI stimulation. This suggested either a negative control of PD-1 expression at the transcriptional level or a defect of PD-1 export at the cell surface in these specific T cell clones. We further explored the expression of the PD-1 gene in these T cell clones at rest and after stimulation.

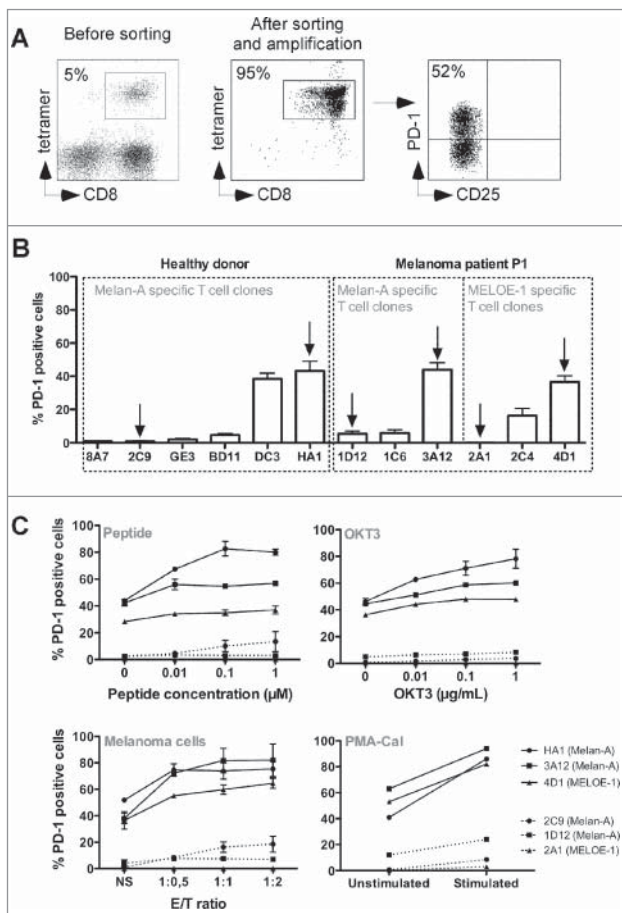


**Figure 1.** PD-1 expression on melanoma-specific T cells clones. (A). Example of specificity and PD-1 expression on Melan-A-specific T cells.  $10^7$  PBMC from a melanoma patient were stimulated in 96-well plates ( $2 \times 10^5$  cells/well) during 14 d with  $1 \mu\text{M}$  of Melan-A<sub>27L</sub> peptide. Melan-A-specific T cells (left panel) were sorted with Chim-AvT dynabeads coated with HLA-A2-peptide monomers and amplified on allogeneic irradiated feeders cells. After 16 d, the specificity (middle panel) and PD-1 expression (right panel) on resting T cells was assessed by a quadruple labeling using tetramer, anti-CD8, anti-CD25 and anti-PD-1 antibodies. (B). Stability of PD-1 expression profile on resting antigen-specific T cell clones. Melan-A and MELOE-1-specific T cell clones were derived from sorted T cell populations by limiting dilution. PD-1 expression on resting T cell clones was assessed by double labeling with anti-PD-1 and anti-CD25 antibodies ( $n = 7$ ). Arrows indicate the T cell clones selected for further characterization. (C). PD-1 expression on specific T cell clones after activation. Specific T cell clones were activated either with a range of Melan-A<sub>27L</sub> or MELOE-1<sub>36-44</sub>-specific peptides, immobilized anti-CD3 Ab (OKT3), HLA-A2 melanoma cell lines or PMA-CaI, for 6 h at  $37^\circ\text{C}$ . Activation and PD-1 expression were assessed by anti-CD25 and anti-PD-1 double labeling ( $n = 3$ ).

### PD-1 expression on melanoma-specific T cell clones is regulated by epigenetic mechanisms

We analyzed PD-1 expression by RT-qPCR in PD-1<sup>pos</sup> and PD-1<sup>neg</sup> T cell clones, at rest and after 6 h of OKT3 stimulation. Activation status was systematically assessed by CD25 labeling. Results were normalized on PD-1 expression, at rest, in the Melan-A-specific T cell clone HA1. As illustrated in Fig. 2A, at rest (white bars), we could not detect PD-1 expression in PD-1<sup>neg</sup> T cell clones (2C9, 1D12 and 2A1), whereas PD-1 mRNA was already present in PD-1<sup>pos</sup> T cell clones (HA1, 3A12 and 4D1). Upon stimulation (gray bars), PD-1 relative expression increased in PD-1<sup>pos</sup> T cell clones, whereas it remained hardly detectable in PD-1<sup>neg</sup> ones. These results are in accordance with those obtained by flow cytometry, suggesting that the absence of PD-1 expression in PD-1<sup>neg</sup> T cell clones was mainly due to a negative transcriptional control. We thus investigated the methylation status of *PDCDI* gene promoter<sup>21,22</sup> on both types of T cell clones by bisulfite sequencing methylation

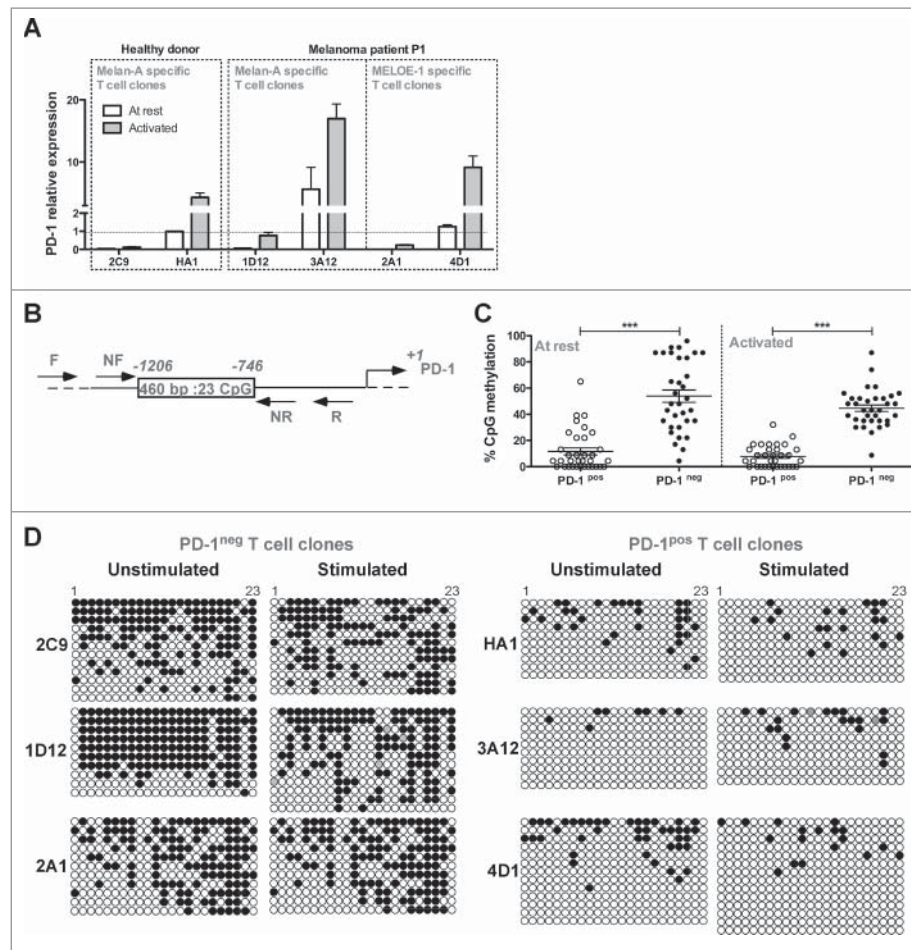


**Figure 2.** Transcriptional regulation of PD-1 expression on T cell clones. (A). PD-1 relative expression measured by RT-qPCR. PD-1 relative expression was measured on resting T cell clones (white bars) or after 6 h of activation with 1  $\mu\text{g}/\text{mL}$  of OKT3 Ab (gray bars). PD-1 relative expression was normalized to the expression of two house-keeping genes (RPLP0 and cyclophilin) and on PD-1 expression measured in resting HA1 T cell clone ( $n = 2$ ). (B). Schematic representation of the PD-1 transcriptional regulatory region. Box represents the 460 bp region containing the 23 CpG analyzed, between  $-1206$  and  $-769$  positions. Arrows indicate the approximate location of the primers (external and nested primers) used for bisulfite sequencing analysis. (C). Global methylation of the regulatory region of *PD-1* gene. Global percentages of methylation (mean  $\pm$  SEM) of the 23 CpG of the PD-1 regulatory region were calculated on at least 33 sequences derived from PD-1<sup>pos</sup> (white circles) and PD-1<sup>neg</sup> (black circles) T cell clones, at rest and after 6 h of activation with OKT3 (1  $\mu\text{g}/\text{mL}$ ). Statistical analyses were performed using a non-parametric Mann-Whitney  $t$  test, to globally compare PD-1<sup>pos</sup> and PD-1<sup>neg</sup> T cell clones ( $***p < 0.001$ , two-tailed  $p$  value). (D). Individual bisulfite sequencing methylation analysis. Bisulfite sequencing of the PD-1 regulatory region was performed on PD-1<sup>neg</sup> and PD-1<sup>pos</sup> T cell clones. DNA treated by bisulfite conversion was amplified, cloned and sequenced. Each line represents an individual clone picked for sequencing. Filled circles represent methylated cytosines and open circles unmethylated ones.

analysis of the 23 CpG nucleotides present in the PD-1 conserved regulatory region (Fig. 2B). Globally, at rest and after TCR stimulation, PD-1<sup>neg</sup> T cell clones exhibited a significantly higher proportion of methylated CpG dinucleotides than PD-1<sup>pos</sup> T cell clones (Fig. 2C). Fig. 2D illustrates the methylation status of each CpG position, and shows that most CpG nucleotides displayed differences in methylation status between PD-1<sup>neg</sup> and PD-1<sup>pos</sup> clonotypes, especially from positions 15 to 21. Upon TCR stimulation, the methylation status of the regulatory region only slightly decreased in one PD-1<sup>neg</sup> T cell clones (1D12, Fig. 2D), an observation consistent with the low PD-1 expression observed by qPCR in this T cell clone after stimulation (Fig. 2A). These data underlined marked differences in the epigenetic regulation program of the *PDCD1* gene, among an antigen-specific T cell repertoire. This epigenetic regulation appears to be the major regulator of PD-1 expression on melanoma-specific T cells. We further explored the reactivity and affinity of these T cell clones.

### PD-1<sup>neg</sup>-specific T cell clones exhibit lower avidity than PD-1<sup>pos</sup> clones

In order to compare the reactivity of PD-1<sup>pos</sup> and PD-1<sup>neg</sup> melanoma-specific T cell clones against natural targets expressing or not a PD-1 ligand, we stably transfected the TAP-deficient T2 cell line and a HLA-A2<sup>+</sup> melanoma cell line (M113) expressing Melan-A and MELOE-1 antigens<sup>20,23</sup> with a PD-L1 expression plasmid. The selected cell lines stably expressed PD-L1 (Fig. 3A) and the PD-L1<sup>pos</sup> melanoma cell line exhibited similar levels of antigens and co-stimulation molecules (HLA-A2, ICAM-1, LFA-3) as compared to the wild-type cell line (Fig. 3B). The reactivity of T cell clones was measured against wild type and transfected cell lines by an IFN $\gamma$ -specific ELISA test, after a 6 h activation period (Fig. 3C). As expected, IFN $\gamma$  production by Melan-A-specific PD-1<sup>neg</sup> T cell clones (2C9 and 1D12) was not altered by PD-L1 expression on melanoma cells (left panel) whereas IFN $\gamma$  production by PD-1<sup>pos</sup> T cell clones (specific for Melan-A and MELOE-1) was substantially decreased upon activation with PD-L1 expressing melanoma cell line (right panel).

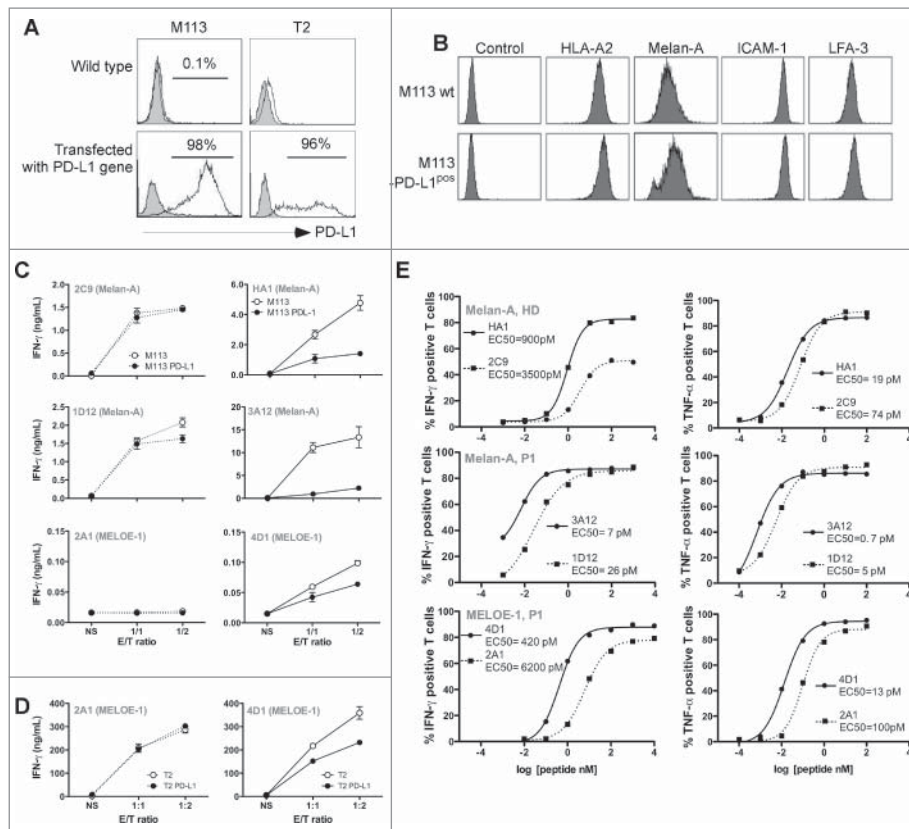


**Figure 3.** Reactivity and affinity of PD-1<sup>pos</sup> and PD-1<sup>neg</sup> T cell clones. (A). Flow cytometric analysis of PD-L1 expression on M113 (left panel) and T2 (right panel) cell lines wild type and stably transfected with a PD-L1 coding expression vector. The filled histograms represent negative control staining while the over-laid empty histograms show staining with a PE-conjugated anti-PD-L1 Ab (clone MIH1, BD Biosciences). (B). Expression of HLA-A2 (clone BB7.2, BD Biosciences), Melan-A (clone A103, Dako, Denmark), ICAM-1 (CD54, clone HA58, BD Biosciences) and LFA-3 (CD58, clone 1C3, BD Biosciences) on M113 (upper panel) and M113-PD-L1<sup>pos</sup> (lower panel) cell lines. All the antibodies, unless A103 Ab were PE-conjugated. For Melan-A intracellular staining, cells were fixed, permeabilized, incubated with A103 Ab, and stained with PE-conjugated goat Fab'2 anti-mouse IgG secondary Ab (Beckman Coulter, France). (C). IFN $\gamma$  production of PD-1<sup>neg</sup> and PD-1<sup>pos</sup> T cell clones in response to melanoma cell lines. IFN $\gamma$  production was measured by ELISA (n = 2) in supernatants of PD-1<sup>neg</sup> (left column, dotted lines) and PD-1<sup>pos</sup> (right column, solid lines) T cell clones after 6 h of activation with M113 melanoma cell line (white circles) or M113-PD-L1<sup>pos</sup> melanoma cell line (black circles). (D). IFN $\gamma$  production of PD-1<sup>neg</sup> and PD-1<sup>pos</sup> MELOE-1-specific T cell clones in response to T2 cells loaded with the MELOE-1<sub>36-44</sub> peptide. IFN $\gamma$  production was measured by ELISA (n = 2) in supernatants of PD-1<sup>neg</sup> (left panel, dotted lines) and PD-1<sup>pos</sup> (right panel, solid lines) MELOE-1-specific T cell clones after a 6-h-activation period with peptide-loaded T2 cells (white circles) or peptide-loaded T2-PD-L1<sup>pos</sup> cells (black circles). (E). Avidities of PD-1<sup>neg</sup> and PD-1<sup>pos</sup> Melan-A and MELOE-1-specific T cell clones. T cell clones' avidities (PD-1<sup>neg</sup>, dotted lines and PD-1<sup>pos</sup>, solid lines) were evaluated by measuring IFN $\gamma$  (left panel) and TNF- $\alpha$  production (right panel) in response to T2 cells loaded either with a range of Melan-A<sub>A27L</sub> peptide or MELOE-1<sub>36-44</sub> peptides, at an E:T ratio of 1:2. Cytokine production was evaluated by intracellular labeling with antibodies specific for IFN $\gamma$  or TNF- $\alpha$  (gated on CD8<sup>+</sup> T cells).

Interestingly, we observed that, globally, Melan-A-specific PD-1<sup>pos</sup> T cell clones produced higher levels of IFN $\gamma$  compared to PD-1<sup>neg</sup> clones. Concerning the pair of MELOE-1 specific T cell clones, we did not observe any IFN $\gamma$  production by the PD-1<sup>neg</sup> T cell clone (2A1) when compared to the PD-1<sup>pos</sup> one (4D1). This suggested that the number of specific HLA-peptide complexes naturally presented by the M113 melanoma cell line was too low to activate the 2A1 specific T cell clone, probably due to its low avidity. We thus retested the reactivity of the two MELOE-1-specific T cell clones on TAP-deficient T2 cells stably transfected or not with PD-L1, and loaded with 10  $\mu$ M of MELOE-1<sub>36-44</sub> peptide. Both clones produced IFN $\gamma$  upon stimulation with peptide-pulsed T2 cells but only the reactivity of 4D1 T cell clone (PD-1<sup>pos</sup>) was affected by PD-L1 expression on T2 cells (Fig. 3D). As observed for Melan-A-specific T cell clones, the PD-1<sup>pos</sup> T cell clone (4D1) was slightly more reactive than the PD-1<sup>neg</sup> one (2A1), in terms of global IFN $\gamma$  production on loaded wild-type T2 cells. Taken together, these results suggested that PD-1<sup>pos</sup>-specific T cell clones may be of higher avidity than PD-1<sup>neg</sup> ones.

We thus formally tested the avidity of these different T cell clones on T2 cells loaded with a range of specific peptides (Fig. 3E). For each pair of specific T cell clones, the PD-1<sup>pos</sup> clone (solid line) exhibited a higher functional avidity than the PD-1<sup>neg</sup> one (dotted line), as evidenced by EC50 values calculated for IFN $\gamma$  and TNF- $\alpha$  production, that were from 4 to 15 times lower for IFN $\gamma$  production (left panel), and from 4 to 7 times lower for TNF- $\alpha$  production (right panel). All these differences were statistically significant, with  $p < 0.0001$  for HA1 vs. 2C9 and 4D1 vs. 2A1 T cell clones for both functions, and with  $p < 0.05$  for 1D12 vs. 3D12 for IFN $\gamma$  production and  $p < 0.001$  for TNF- $\alpha$  production. Therefore, PD-1<sup>neg</sup>-specific T cell clones naturally present within an endogenous repertoire exhibit lower avidity than PD-1 expressing T cell clones and would represent suboptimal effectors. We thus sought to investigate at the polyclonal level the impact of PD-1 blockade during the production process of specific T cells on repertoire diversity and functional avidity of amplified melanoma-specific T cells.

### Existence of PD-1<sup>neg</sup>-specific T cell clones of low functional avidity within melanoma TIL

In order to exclude that the existence of T cell clones unable to express PD-1 was not artificially induced by peptide stimulation *in vitro*, we looked for such T cell clones within Melan-A-specific TIL from two melanoma patients, after cloning by limiting dilution.<sup>24</sup> We measured PD-1 expression on three Melan-A-specific T cell clones derived from M180 melanoma tumor and two specific TIL clones from M199 tumor. As shown in Fig. 4A, we found two TIL clones unable to express PD-1 after OKT3 stimulation from both populations (M180.51 and M199.17). We further compared functional avidities of these TIL clones measuring CD107a degranulation and documented in both cases, that PD-1<sup>neg</sup> TIL clones exhibited a significantly much lower functional avidity than their PD-1<sup>pos</sup> counterparts ( $p < 0.0001$ ) (Fig. 4B).

### The addition of PD-1-blocking antibody during the amplification process of Melan-A-specific T cells enhanced their proliferation and modifies specific T cell repertoire

We first compared the amplification rates of Melan-A-specific T lymphocytes expanded according to the standard peptide-stimulation step or to a modified procedure in which an anti-PD-1 blocking Ab was added together with the peptide. This comparison was performed on PBMC derived from two HLA-A2 healthy donors and three melanoma patients. The absolute number of Melan-A-specific T cells (calculated from the total number of T cells and the fraction of tetramer-positive lymphocytes at the end of the peptide stimulation step) was from 2 to 9 times greater in this new culture condition (Fig. 5A, hatched bars), as compared to the control condition (white bars). Thus, PD-1 blockade enhances the specific T

cell expansion induced by peptide stimulation of PBMC, derived either from healthy donors or melanoma patients.

This increased proliferation of specific T lymphocytes prompted us to compare the diversity of the specific T cell repertoire amplified in both conditions. To this aim, specific T cells were sorted as previously described,<sup>18</sup> and amplified with or without anti-PD-1-blocking Ab. After this amplification step, recovered T lymphocytes were fully specific of Melan-A antigen as documented by specific tetramer labeling and rather polyclonal as shown in Fig. 5B illustrating V $\beta$  subfamilies representing more than 5% of specific T cells. Melan-A-specific T cell repertoire was significantly modified when T cells were produced in the presence of anti-PD-1 Ab (hatched bars), as compared to the control condition (white bars). For each donor or patient, we observed the specific proliferation of one to two V $\beta$  subfamilies that were under-represented or absent in the control condition. This increased proliferation appears detrimental to other populations preferentially expanded in the control condition.

Concerning healthy donor HD49, Melan-A-specific T cell repertoire is polyclonal in both conditions, with V $\beta$ 14 lymphocytes as the dominant subfamily in the control condition (28%) and V $\beta$ 7.1 (6.5%) and V $\beta$ 16 (6%) subfamilies specifically amplified in the “anti-PD-1” condition. Specific T cell repertoire was much narrower in HD52 donor, with V $\beta$ 14 subfamily shared in both conditions, and V $\beta$ 23 and V $\beta$ 7.2 subfamilies specifically amplified respectively in the control and “anti-PD-1” conditions. Thus, blocking PD-1 pathway during the amplification process of Melan-A-specific T cells appeared to modify specific T cell repertoire. We then conducted the same experiments on PBMC derived from three melanoma patients and confirmed this result.

Indeed, for the patient P2, Melan-A-specific T cells were globally poorly polyclonal, with a dominant (86%) V $\beta$ 13.1 subfamily in the control condition and two distinct dominant V $\beta$  subtypes in the “anti-PD-1” condition: V $\beta$ 13.2 (15%) and V $\beta$ 14 (75%). Melan-A-specific T cells from patient P3 were more polyclonal with common and well-represented V $\beta$  subtypes in both conditions (V $\beta$ 13.1 and V $\beta$ 14). Nonetheless, V $\beta$ 3 and V $\beta$ 17 lymphocytes representing respectively 28% and 16% of Melan-A-specific T cells in the control condition were almost absent in the “anti-PD-1” condition. Conversely, Melan-A-specific V $\beta$ 23 T cells were specifically amplified (16%) in this latter culture condition. Finally, specific repertoire differences were even more pronounced for patient P4, with a polyclonal repertoire for the control condition, and a major amplification of V $\beta$ 20 Melan-A-specific T cells (85%) for the “anti-PD-1” condition.

As the use of an anti-PD-1-blocking Ab in our selection and amplification procedure clearly favored the proliferation of peculiar V $\beta$  subfamilies, we decided to compare the avidity of these subpopulations to that of V $\beta$  subtypes preferentially expanded in the control condition (indicated by arrows in Fig. 5B).

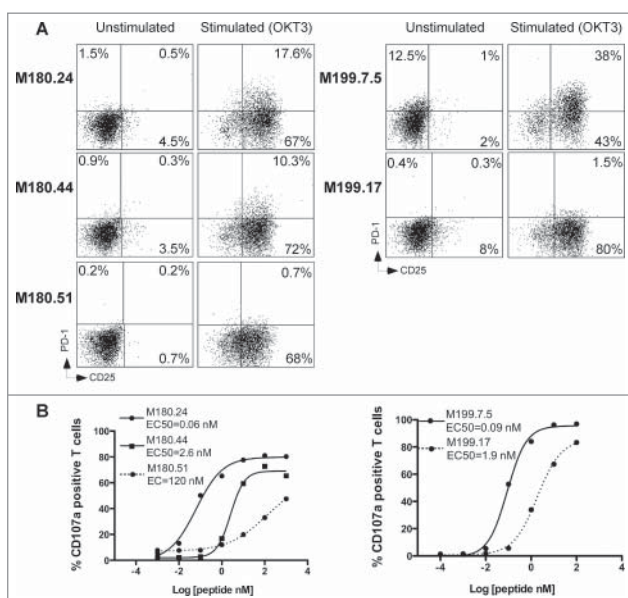


**Figure 4.** PD-1 expression and functional avidity of Melan-A-specific T cell clones derived from melanoma TIL. (A). CD25-PD-1 labeling of TIL clones, at rest and after OKT3 stimulation (1  $\mu$ g/mL, 6 h at 37°C). (B) Functional avidities of PD-1<sup>neg</sup> (dotted lines) and PD-1<sup>pos</sup> TIL clones (solid lines) were evaluated by measuring CD107a membrane expression in response to T2 cells loaded with a range of Melan-A<sub>27L</sub> peptide, at an E:T ratio of 1:2. CD107a membrane expression was evaluated by double staining with anti-CD8 and CD107a monoclonal antibodies.

### The addition of PD-1-blocking antibody favors the amplification of high-avidity clonotypes

We tested the affinity of V $\beta$  subfamilies specifically enriched in the two culture conditions on T2 cells loaded with a range of

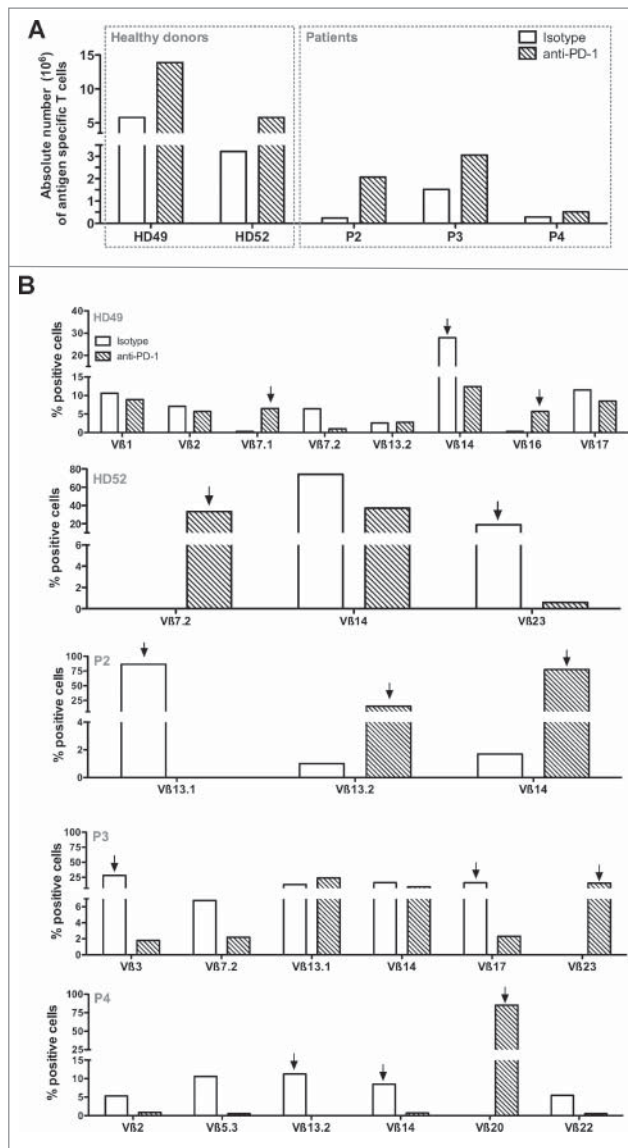


**Figure 5.** Amplification rates and Melan-A-specific T cell diversity in presence of anti-PD-1 blocking antibody. (A). Absolute number of Melan-A-specific T cells after the step of PBMC-peptide stimulation.  $10^7$  PBMC from HLA-A2 healthy donors and melanoma patients were stimulated in 96-well plates ( $2 \times 10^5$  cells/well) during 14 d with  $1 \mu\text{M}$  of Melan-A<sub>A27L</sub> peptide, in presence of  $10 \mu\text{g}/\text{mL}$  of anti-PD-1 Ab (hatched bars) or with  $10 \mu\text{g}/\text{mL}$  of control IgG (white bars). At the end of the stimulation period, the absolute number of Melan-A-specific T cells was calculated from the total number of expanded T lymphocytes and the percentage of tetramer positive cells. (B). Analysis of the V $\beta$  repertoire of sorted and amplified Melan-A-specific T cells from stimulated PBMC. A panel of 24 anti-V $\beta$  antibodies was used. Empty histograms represent Melan-A-specific repertoire expanded in the control condition, and hatched histograms represent the repertoire amplified upon culture in the presence of anti-PD-1 Ab. Arrows indicate V $\beta$  subfamilies specifically amplified in one or the other of these two culture conditions, used for further analyses.

Melan-A<sub>A27L</sub> peptide, using double staining with a specific anti-V $\beta$  Ab together with IFN $\gamma$  (Fig. 6, left panel), TNF- $\alpha$  (middle panel) or CD107a labeling (right panel). Solid lines represent V $\beta$  subpopulations specifically expanded with anti-PD-1 Ab and dotted lines V $\beta$  subpopulations preferentially expanded in the control condition. For healthy donors (HD49 and HD52) V $\beta$  subfamilies selected in the presence of anti-PD-1 mAb exhibited better functional avidities than those amplified in the control condition with a difference in EC50 ranging from 2 to 15 for each tested function (Fig. 6 and Table 1), reaching

statistical significance for V $\beta$ 16 (IFN $\gamma$  and CD107a) and V $\beta$ 7.1 (CD107a) subfamilies from HD49 and for V $\beta$ 7.2 (for the three tested functions) from HD52. Concerning patient P2, the V $\beta$ 14 subpopulation (amplified in the presence of anti-PD-1 Ab and representing 78% of Melan-A-specific T cells) exhibited a slightly better EC50 than the other V $\beta$  families, only significant for IFN $\gamma$  production (Fig. 6 and Table 1). V $\beta$ 23-specific T lymphocytes specifically expanded from patient P3 in the presence of anti-PD-1 mAb also exhibited a significantly better EC50 than the V $\beta$ 3 subpopulation expanded without anti-PD-1 for the three tested functions, and then V $\beta$ 17 subpopulation for CD107a degranulation and TNF- $\alpha$  production. Finally, V $\beta$ 20 lymphocytes, largely represented (85%) in the “anti-PD-1” condition for patient P4, also had a significantly better EC50 than V $\beta$ 14 (for the three functions) and V $\beta$ 13.2 (for CD107a and TNF- $\alpha$  production) lymphocytes amplified in the control condition (Fig. 6 and Table 1).

Taken together, these results strongly suggest that PD-1 blockade favors the expansion of PD-1<sup>pos</sup> specific T lymphocytes with higher avidity, probably because in the absence of PD-1 blocking Ab, PD-1 signaling inhibits the proliferation of such T lymphocytes.

## Discussion

PD-1 has been largely described as a strong negative regulator of tumor-specific T cells, but also as a marker of activated effector T cells. As the induction of PD-1 after T cell activation is positively correlated with the strength of TCR signaling, we sought to explore the link between antigen T cell avidity and PD-1 expression. We documented for the first time the existence of melanoma-specific T cell clones constitutively unable to express PD-1, at rest and after activation. In these T cell clones, PD-1 expression was controlled at the transcriptional level by a stable methylation pattern of PD-1 gene promoter, that could not be overcome by stimulation (Figs 1 and 2). It has been previously demonstrated in chronic infection models, that PD-1 promoter methylation controls PD-1 expression after TCR activation.<sup>22</sup> In PD-1<sup>hi</sup> HIV-specific CD8<sup>+</sup> T cells, the low methylation rate of PD-1 promoter remained a stable feature, even when the viral load was controlled for long periods, suggesting that the epigenetic program at the PD-1 locus could determine PD-1 expression profile.<sup>21</sup> Furthermore, it has been recently reported the upregulation of PD-1 expression on T cells from patients with myelodysplastic syndrome treated with hypomethylating agents.<sup>25</sup> It has also been demonstrated that NFAT transcription factors regulate the expression of the PD-1 gene by direct binding to the PD-1 promoter,<sup>26,27</sup> and so we expect that hypermethylation of the PD-1 promoter region should prevent NFAT fixation and subsequent gene transcription. In support of this hypothesis, a consensus NFAT binding sequence located between CpG positions 17 and 18, was consistently hypermethylated in PD-1<sup>neg</sup> T cell clones (Fig. 2D). Surprisingly, this marked difference in PD-1 expression between these two types of T cell clones was not associated with additional differences in the expression of other activation or exhaustion markers (Table S1). Indeed, it has been recently described in a model of PD-1 deficient mice, that the absence of PD-1 led to the accumulation of exhausted CD8<sup>+</sup> T cells, in

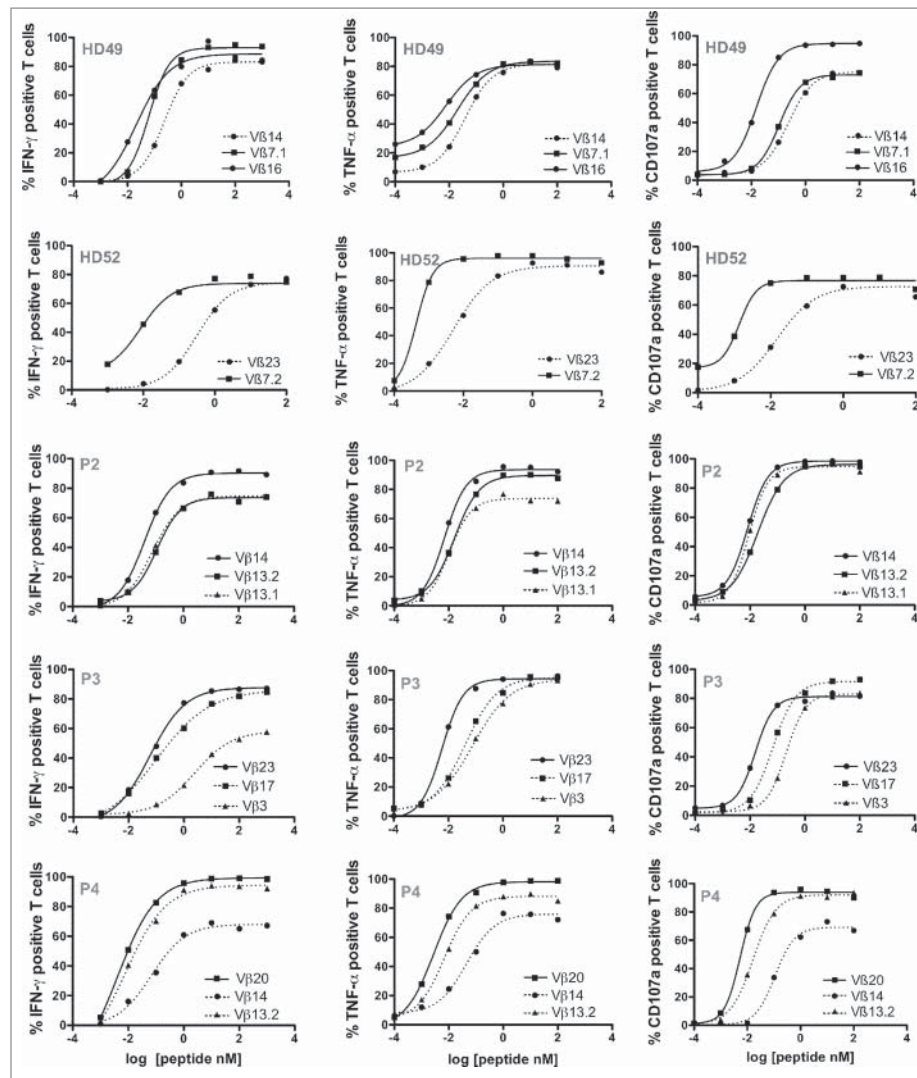


**Figure 6.** Functional avidities of the different V $\beta$  subfamilies specifically expanded in the two culture conditions. Avidities of specific V $\beta$  subfamilies amplified in the control condition (dotted lines) or in the presence of anti-PD-1 Ab (solid lines) were evaluated by measuring IFN $\gamma$  (left panel) and CD107a membrane expression (right panel) in response to T2 cells loaded with a range of Melan-A<sub>27L</sub> peptide, at an E:T ratio of 1:2. Cytokine production and CD107a membrane expression were evaluated by double staining with specific anti-V $\beta$  antibodies and intracellular or membrane labeling.

the context of chronic viral infection, with a shift toward a high expression of the transcription factor Eomes compared to T-bet.<sup>28</sup> We did not observe either any difference in T-bet or Eomes expression between PD-1<sup>pos</sup> and PD-1<sup>neg</sup> melanoma-specific T cell clones (data not shown), suggesting that the absence of PD-1 on human memory T cell clones does not have the same impact than genetic PD-1 deficiency in the context of viral infection.

From a functional perspective, reactivity of PD-1<sup>neg</sup> T cell clones was, as expected, not affected by PD-L1 expression on melanoma cell lines, but their global reactivity was lower than that of PD-1<sup>pos</sup> clones (Figs 3C and D). We further documented the higher avidity of PD-1<sup>pos</sup> T cell clones on T2 cells loaded with a range of specific peptides (Fig. 3E). These differences in functional avidities of PD-1<sup>pos</sup> and PD-1<sup>neg</sup> T cells naturally present in the periphery could be explained by positive and negative selection events. Indeed, since PD-L1 is expressed in the thymus, the interaction PD-1/PDL-1 shapes antigen-specific T cell repertoires. As demonstrated in a

mouse model, the absence of PD-1 on thymocytes leads to the positive selection of low affinity thymocytes and to a greater deletion of high-affinity thymocytes by negative selection.<sup>29,30</sup> In our model, we hypothesize that low-avidity PD-1<sup>neg</sup> melanoma-specific T cell clonotypes pass positive selection while high-avidity PD-1<sup>neg</sup> specific T cell clonotypes are eliminated by negative selection. Accordingly, the endogenous PD-1<sup>neg</sup> specific T cell repertoire for any given antigen should be of lower avidity than the PD-1<sup>pos</sup> repertoire. In order to strengthen these observations and to exclude any artifactual mechanisms due to the step of peptide stimulation of PBMC, we looked for PD-1<sup>neg</sup> T cell clones derived from melanoma TILs. We both confirmed the presence within melanoma TILs of Melan-A-specific T cell clones unable to express PD-1, and that these T cell clones exhibited a lower functional avidity than their PD-1<sup>pos</sup> counterparts.

We thus investigated the impact of PD-1 blockade during the production process of Melan-A-specific T cells, on repertoire diversity and T cell avidity. We first reported the benefit

of blocking PD-1 signalization during the peptide stimulation step on the amplification rate of specific T cells (Fig. 5A). Such an increase in the amplification of melanoma-specific T cells resulting from blocking PD-1 signalization had been previously described on the *in vitro* expansion of Melan-A and gp100-specific T lymphocytes, derived from melanoma patient blood.<sup>31</sup> To go further, we investigated whether this increased proliferation concerned the whole Melan-A repertoire or only specific T cell clonotypes. Starting from two healthy donors and three melanoma patients, we showed that Melan-A-specific T cell repertoire was clearly biased by the use of anti-PD-1 Ab *in vitro* (Fig. 5B). Therefore, blocking PD-1 signalization not only increased the amplification of Melan-A-specific T cells but also shaped this specific repertoire. We further showed that the avidity of specific clonotypes amplified with anti-PD-1 Ab was better than those of clonotypes amplified in the control condition (Fig. 6). This suggests that PD-1 blocking preferentially favors the amplification of high-avidity-specific T cells, which naturally express high levels of PD-1 upon activation and whose proliferation is inhibited by PD-1 signaling in standard conditions. These results are consistent with previous studies reporting that melanoma reactive TIL were enriched in PD-1<sup>pos</sup> CD8<sup>+</sup> T lymphocytes,<sup>32</sup> and that PD-1, in addition to its inhibitory functions, could be a useful biomarker to identify tumor-specific T cell repertoire in melanoma, including mutated neo-antigen-specific CD8<sup>+</sup> lymphocytes.<sup>11,17</sup> Our findings strengthen the hypothesis that PD-1 expression is a robust marker for highly reactive specific T lymphocytes. Furthermore, as PD-1 blockade favors the expansion of highly reactive T cells *in vitro*, the same phenomenon probably occurs *in vivo*, as strongly suggested by a recent study that showed that therapeutic efficacy of PD-1 blockade required pre-existing CD8<sup>+</sup> PD-1<sup>+</sup> T cells inhibited by PD-1/PD-L1 signaling.<sup>16</sup> Thus, we reckon that the immune-follow-up of anti-PD-1-treated patients should include investigating changes in antigen specific repertoire diversity and avidity during the course of the treatment, in addition to the search for neo-antigen-specific T cells potentially associated with a high tumor mutation rate.<sup>17</sup>

Globally these results provide new insights about the molecular mechanisms regulating PD-1 expression in melanoma-specific T cell clones and about the dual role of PD-1 in modulating the diversity and functions of an antigen-specific T cell repertoire. This also offers new prospects for monitoring immune responses of cancer patients treated with anti-PD-1 antibody and for the selection of optimal effector T cells for adoptive cell transfer treatments.

## Material and Methods

### PBMC and cell lines

PBMC were isolated from healthy HLA-A2 donors (Etablissement Français du Sang (EFS), Nantes, France) or from metastatic melanoma patients (Unit of Skin Cancer, Nantes hospital) after written informed consent (Nantes ethic committee, approval number: DC-2011-1399).

The melanoma cell line M113 was established from metastatic tumor fragments in the Unit of Cell therapy of Nantes

**Table 1.** Proportion and EC50 of Melan-A-specific V $\beta$  subfamilies amplified in the two different culture conditions.

	Condition	% <sup>b</sup>	EC50 (pM) <sup>a</sup>		
			IFN $\gamma$	TNF- $\alpha$	CD107a
<b>HD49</b>					
V $\beta$ 16	anti-PD-1	6%	21**	7	15***
V $\beta$ 7.1	anti-PD-1	7%	62	20	110***
V $\beta$ 14	Control	28%	230	35	230
<b>HD52</b>					
V $\beta$ 7.2	anti-PD-1	33%	8**	0.4*	1.4*
V $\beta$ 23	Control	19%	310	5	15
<b>Patient P2</b>					
V $\beta$ 14	anti-PD-1	78%	40*	7	7
V $\beta$ 13.2	anti-PD-1	15%	110	16	12
V $\beta$ 13.1	Control	86%	75	10	7
<b>Patient P3</b>					
V $\beta$ 23	anti-PD-1	16%	60	6	15
V $\beta$ 17	Control	16%	100	43***	68***
V $\beta$ 3	Control	28%	2500***	78***	206***
<b>Patient P4</b>					
V $\beta$ 20	anti-PD-1	85%	4	3	5
V $\beta$ 14	Control	9%	70**	36***	110***
V $\beta$ 13.2	Control	11%	8	7*	16***

<sup>a</sup>EC50 were determined after activation of Melan-A-specific T cell lines by T2 cells loaded with a range of Melan-A<sub>A27L</sub> peptide. The fraction of IFN $\gamma$ , TNF- $\alpha$  and CD107a<sup>pos</sup> cells among a specific V $\beta$  subfamily was evaluated by flow cytometry, by double labeling. <sup>b</sup>The % indicates the proportion of each V $\beta$  subfamily among all Melan-A-specific T cells. Statistical analysis comparing LogEC50 of V $\beta$  subfamilies amplified with and without anti-PD-1 mAb was performed using PRISM software (one-way ANOVA analysis), followed by a Bonferroni's multiple comparison test.

\* $p < 0.05$ ; \*\* $p < 0.01$ ; \*\*\* $p < 0.001$ .

and are registered in the Biocollection PC-U892-NL (CHU Nantes).

The human TAP deficient cell line T2 (174  $\times$  CEM.T2) used as a presenting cell was purchased from the ATCC (CRL-1992). M113 and T2 cell lines stably expressing human PD-L1 were established upon transfection with an eukaryotic expression vector (pCDNA3) bearing human PD-L1 gene (NM 14143.2, Sino Biological, HG10084-UT), using lipofectamine, according to the manufacturer's recommendation (Life technologies, 15338100). Stable transfectants expressing PD-L1 were selected and cultured in medium containing 0.8  $\mu$ g/mL of G418 antibiotic.

### Peptide stimulation of PBMC

PBMC were seeded in 96 well/plates at  $2 \times 10^5$  cells/well in RPMI 1640 medium supplemented with 8% human serum (HS), 50 IU/mL of IL-2 (Proleukin, Novartis) and 10  $\mu$ g/mL of either anti-PD-1 Ab (Clone EH12.2H7, Biolegend, 329912) or IgG1 control isotype (Biolegend, 401404). PBMC were stimulated with 1  $\mu$ M of Melan-A<sub>A27L</sub> peptide (ELAGIGILTV) or 10  $\mu$ M of MELOE-1<sub>36-44</sub> peptide (TLNDECWPA) purchased from Proteogenix. Following stimulation, each microculture was evaluated for the percentage of specific CD8<sup>+</sup> T lymphocytes by double staining with the relevant HLA-peptide tetramer (from the SFR Sante recombinant protein facility) and anti-CD8 mAb (clone BW135/80, Miltenyi Biotec) using a FACS Canto HTS. Microcultures that contained at least 1% of specific T cells were selected, pooled and sorted with the relevant multimer-coated beads.<sup>18</sup>



### Sorting, amplification and cloning of specific T cells

Sorting and amplification of Melan-A and MELOE-1-specific T cells was performed as previously described.<sup>18,23</sup> To isolate and expand Melan-A and MELOE-1-specific T cell clones from specific sorted T cells, we used a limiting dilution cloning method previously described.<sup>33</sup> Melan-A and MELOE-1-specific T cell clones, from microcultures showing greater than 95% probability of monoclonality according to the single-hit Poisson law, were selected on the basis on specific tetramer labeling.

### T cell clones from melanoma TIL

Melan-A-specific T cell clones were derived from two melanoma TIL populations by limiting dilution, as previously described, and clonality was attested by sequencing of TCR  $\alpha$  and  $\beta$  chains.<sup>24</sup>

### Activation of antigen-specific T cells

Phenotypic and functional analyses were performed on resting or activated T cells. Antigen-specific T cells were activated 6 h in 96-well plates with either coated anti-CD3 Ab (clone OKT3, CRL-8001, ATCC) at 1  $\mu$ g/mL, addition of 1  $\mu$ M of Melan-A<sub>A27L</sub> peptide (ELAGIGILTV) or 10  $\mu$ M of MELOE-1<sub>36-44</sub> peptide (TLNDECWPA), co-culture with the M113 melanoma cell line at two effector/target ratios (1/1 and 1/2) or with addition of 1  $\mu$ g/mL of phorbol myristate acetate and calcium ionophore (PMA-CaI, Sigma P8139 and I3909).

### Phenotype and V $\beta$ repertoire of specific T cells

Phenotypic characterization on resting T cell clones was performed on 10<sup>5</sup> T cells labeled with MELOE-1 and Melan-A tetramers (10  $\mu$ g/mL) (Recombinant protein facility, SFR Santé, Nantes, France), anti-CD8 (clone BW135/80, Miltenyi Biotec), anti-CD45RO (clone UCHL1, BD Biosciences), anti-CD27 (clone M-T271, BD Biosciences), anti-CD28 (clone CD28.2, BD Biosciences), anti-CD62L (clone DREG-56, BD Biosciences), anti-PD-1 (clone EH12, BD Biosciences), anti-CTLA-4 (clone BNI3, Miltenyi Biotec), anti-BTLA (clone J168-540, BD Biosciences), anti-Tim-3 (clone F38-2E2, eBiosciences) and anti-CD95 (clone DX2, BD Biosciences) specific antibodies. PD-1 expression (Clone EH12, BD Biosciences) was tested on specific T cell clones or sorted T cells at rest and after activation by quadruple labeling with specific tetramers, anti-CD8 and anti-CD25 (clone M-A251, BD Biosciences), as activation marker. All the antibodies were used at a concentration of 5  $\mu$ g/mL. V $\beta$  diversity of sorted Melan-A-specific T cell lines was analyzed by labeling with 24 anti-V $\beta$  mAbs included in the IOTest Beta Mark TCR V Kit (Beckman-Coulter, IM3497). All the cytometric analyses were performed on a FACS Canto II (BD Biosciences).

### Real-time PCR

Total RNA was extracted from antigen-specific T cells using NucleoSpin RNA II kit (Macherey-Nagel, France). 1  $\mu$ g of total RNA was retrotranscribed using SuperScript III reverse

transcriptase and oligodT (Thermo Fisher Scientific, 18080-044 and 18418-020). Relative quantification of PD-1 and housekeeping genes RPLPO and Cyclophilin-A (Table S2) was performed using brilliant SYBR Green qPCR with an Mx4000 machine (Agilent Technologies). PD-1-specific primers were purchased from Qiagen (catalog number PPH13086G). Thermal cycling was one step at 95°C for 10 min, followed by 40 cycles at 95°C for 30 s and 60°C for 1 min. Duplicate series of 10-fold-diluted cDNA from the Melan-A-specific T cell clone HA1 at rest were used to calculate the efficiency of PCR reaction. Mean threshold cycle (CT) values from duplicate PCR reactions were normalized to mean CT values for the two housekeeping genes from the same cDNA preparations. The relative expression ratio of PD-1 gene was calculated based on the PCR efficiency (E) and the CT deviation between a given cell sample (x) and a reference cell sample (calibrator: HA1 resting T cell clone), expressed in comparison with the mean of the housekeeping genes: ratio = (E target) <sup>$\Delta$  CT target (calibrator - x)</sup>/mean ((E housekeeping) <sup>$\Delta$  CT housekeeping (calibrator - x)</sup>).

### Methylation status analyses

DNA from specific T cells was extracted using QiaAmp DNA mini kit (Qiagen, France). Methyl-Collector Bisulfite modification kit (Active Motif, 55016) was used for DNA conversion. DNA converted samples were amplified by two successive PCR with specific primers (Table S2). Thermal cycles for PCR1 were one step at 95°C for 5 min, followed by 20 cycles at 95°C for 30 s, 63°C for 2 min and 72°C for 1 min 30 s. Thermal cycles for PCR2 were one step at 95°C for 5 min, followed by 20 cycles at 95°C for 30 s, 57°C for 1 min and 72°C for 1 min 30 s. Amplimers were cloned into pSC-B-Amp/Kan vector (Agilent Technologies, 240207) and a minimum of 12 clones for each sample were sequenced (Eurofins scientific).

### Specific T cell avidity and reactivity

IFN $\gamma$  secretion of activated T cells was measured by a specific ELISA assay (Human IFN gamma ELISA Ready-SET-Go, eBioscience, 88-7316-88), after 6 h of activation with either M113 and M113-PD-L1<sup>pos</sup> melanoma cell line or T2 cell line and its T2-PD-L1 transfected counterpart, loaded with 10  $\mu$ M of MELOE-1<sub>36-44</sub> peptide. The relative avidity of T cell clones and sorted T cells was measured by intracellular IFN $\gamma$  and TNF- $\alpha$  production and CD107a membrane expression, in response to T2 cells loaded with a range of specific peptides (E/T ratio 1/2). After a 6-h-stimulation period with peptide-loaded T2 cells, in presence of brefeldin A at 10  $\mu$ g/mL (Sigma, B7651), T cells were labeled with PE-conjugated specific anti-V $\beta$  antibodies (Beckman Coulter) and fixed with PBS 4% paraformaldehyde (VWR, 100504-858). Lymphocytes were then stained for cytokine production using APC conjugated anti-TNF- $\alpha$  (clone cA2, Miltenyi Biotec) and anti-IFN $\gamma$  (clone 45-15, Miltenyi Biotec). Concerning CD107a labeling, specific T cells were stimulated at a E/T ratio of 1/2 with peptide loaded T2 cells for 4 h at 37°C in the presence of APC-conjugated mAb specific for CD107a (clone H4A3, BD Biosciences). T cells were then stained with selected anti-V $\beta$  antibodies (Beckman Coulter) and analyzed by flow cytometry.

## Statistical analyses

Statistical analyses were conducted to compare the percentages of global methylation of the 23 CpG dinucleotides of the PD-1 regulatory region, between PD-1<sup>pos</sup> and PD-1<sup>neg</sup> T cell clones (at least 33 sequences analyzed in each group), and PD-1<sup>pos</sup> and PD-1<sup>neg</sup> Melan-A-specific sorted T cells (at least 12 sequences analyzed in each group). These analyses were performed using a non-parametric Mann–Whitney t test, with two-tailed *p* value. We performed statistical analyses for the comparisons of EC50 for T cell clones and Melan-A-specific Vβ subfamilies derived from stimulated PBMC. Log EC50 for each pair of clones were compared using the extra sum-of-squares F test. When more than two populations were compared (M180 TIL clones and Vβ subfamilies amplified in the two culture conditions), we used a one-way ANOVA analysis, followed by a Bonferroni's multiple comparison test. All these analyses were performed using PRISM software.

## Disclosure of potential conflicts of interest

No potential conflicts of interest were disclosed.

## Acknowledgments

We thank Dr Y. Delneste and M. Bonneville for critical reading of the manuscript, and Dr Moreau-Aubry for expert assistance in bisulfite experiments. We thank the Recombinant Protein Facility (SFR Sante) for HLA-A2/peptide monomers' production and the Cytometry Facility "CytoCell" (SFR Sante) for expert technical assistance.

## Funding

This work was performed in the context of the LabEX IGO program supported by the National Research Agency via the investment of the future program ANR-11-LABX-0016-01. Sylvain Simon was supported by a specific thesis allocation from the LabEx IGO program. This work was also supported by grants from the « Ligue contre le Cancer, Comite 44 » and the canceropole Grand-Ouest.

## References

- Kamphorst AO, Ahmed R. Manipulating the PD-1 pathway to improve immunity. *Curr Opin Immunol* 2013; 25:381-8; PMID:23582509; <http://dx.doi.org/10.1016/j.coi.2013.03.003>
- Moll M, Kuylensstierna C, Gonzalez VD, Andersson SK, Bosnjak L, Sonnerborg A, Quigley MF, Sandberg JK. Severe functional impairment and elevated PD-1 expression in CD1d-restricted NKT cells retained during chronic HIV-1 infection. *Eur J Immunol* 2009; 39:902-11; PMID:19197939; <http://dx.doi.org/10.1002/eji.200838780>
- Riley JL. PD-1 signaling in primary T cells. *Immunol Rev* 2009; 229:114-25; PMID:19426218; <http://dx.doi.org/10.1111/j.1600-065X.2009.00767.x>
- Nishimura H, Nose M, Hiai H, Minato N, Honjo T. Development of lupus-like autoimmune diseases by disruption of the PD-1 gene encoding an ITIM motif-carrying immunoreceptor. *Immunity* 1999; 11:141-51; PMID:10485649; [http://dx.doi.org/10.1016/S1074-7613\(00\)80089-8](http://dx.doi.org/10.1016/S1074-7613(00)80089-8)
- Nishimura H, Okazaki T, Tanaka Y, Nakatani K, Hara M, Matsumori A, Sasayama S, Mizoguchi A, Hiai H, Minato N et al. Autoimmune dilated cardiomyopathy in PD-1 receptor-deficient mice. *Science* 2001; 291:319-22; PMID:11209085; <http://dx.doi.org/10.1126/science.291.5502.319>
- Keir ME, Butte MJ, Freeman GJ, Sharpe AH. PD-1 and its ligands in tolerance and immunity. *Annu Rev Immunol* 2008; 26:677-704; PMID:18173375; <http://dx.doi.org/10.1146/annurev.immunol.26.021607.090331>
- Sheppard KA, Fitz LJ, Lee JM, Benander C, George JA, Wooters J, Qiu Y, Jussif JM, Carter LL, Wood CR et al. PD-1 inhibits T-cell receptor induced phosphorylation of the ZAP70/CD3zeta signalosome and downstream signaling to PKCtheta. *FEBS Lett* 2004; 574:37-41; PMID:15358536; <http://dx.doi.org/10.1016/j.febslet.2004.07.083>
- Dong H, Strome SE, Salomao DR, Tamura H, Hirano F, Flies DB, Roche PC, Lu J, Zhu G, Tamada K et al. Tumor-associated B7-H1 promotes T-cell apoptosis: a potential mechanism of immune evasion. *Nat Med* 2002; 8:793-800; PMID:12091876; <http://dx.doi.org/10.1038/nm0902-1039c>
- Zitvogel L, Kroemer G. Targeting PD-1/PD-L1 interactions for cancer immunotherapy. *Oncoimmunology* 2012; 1:1223-5; PMID:23243584; <http://dx.doi.org/10.4161/onci.21335>
- Ahmadzadeh M, Johnson LA, Heemskerck B, Wunderlich JR, Dudley ME, White DE, Rosenberg SA. Tumor antigen-specific CD8 T cells infiltrating the tumor express high levels of PD-1 and are functionally impaired. *Blood* 2009; 114:1537-44; PMID:19423728; <http://dx.doi.org/10.1182/blood-2008-12-195792>
- Gros A, Robbins PF, Yao X, Li YF, Turcotte S, Tran E, Wunderlich JR, Mixon A, Farid S, Dudley ME et al. PD-1 identifies the patient-specific CD8(+) tumor-reactive repertoire infiltrating human tumors. *J Clin Invest* 2014; 124:2246-59; PMID:24667641; <http://dx.doi.org/10.1172/JCI73639>
- Hamid O, Robert C, Daud A, Hodi FS, Hwu WJ, Kefford R, Wolchok JD, Hersey P, Joseph RW, Weber JS et al. Safety and tumor responses with lambrolizumab (anti-PD-1) in melanoma. *N Engl J Med* 2013; 369:134-44; PMID:23724846; <http://dx.doi.org/10.1056/NEJMoa1305133>
- Topalian SL, Sznol M, McDermott DF, Kluger HM, Carvajal RD, Sharfman WH, Brahmer JR, Lawrence DP, Atkins MB, Powderly JD et al. Survival, durable tumor remission, and long-term safety in patients with advanced melanoma receiving nivolumab. *J Clin Oncol* 2014; 32:1020-30; PMID:24590637; <http://dx.doi.org/10.1200/JCO.2013.53.0105>
- Wolchok JD, Kluger H, Callahan MK, Postow MA, Rizvi NA, Leschkhin AM, Segal NH, Ariyan CE, Gordon RA, Reed K et al. Nivolumab plus ipilimumab in advanced melanoma. *N Engl J Med* 2013; 369:122-33; PMID:23724867; <http://dx.doi.org/10.1056/NEJMoa1302369>
- Taube JM, Klein A, Brahmer JR, Xu H, Pan X, Kim JH, Chen L, Pardoll DM, Topalian SL, Anders RA. Association of PD-1, PD-1 ligands, and other features of the tumor immune microenvironment with response to anti-PD-1 therapy. *Clin Cancer Res* 2014; 20:5064-74; PMID:24714771; <http://dx.doi.org/10.1158/1078-0432.CCR-13-3271>
- Tumeh PC, Harview CL, Yearley JH, Shintaku IP, Taylor EJ, Robert L, Chmielowski B, Spasic M, Henry G, Ciobanu V et al. PD-1 blockade induces responses by inhibiting adaptive immune resistance. *Nature* 2014; 515:568-71; PMID:25428505; <http://dx.doi.org/10.1038/nature13954>
- Rizvi NA, Hellmann MD, Snyder A, Kvistborg P, Makarov V, Havel JJ, Lee W, Yuan J, Wong P, Ho TS et al. Cancer immunology. Mutational landscape determines sensitivity to PD-1 blockade in non-small cell lung cancer. *Science* 2015; 348:124-8; PMID:25765070; <http://dx.doi.org/10.1126/science.aaa1348>
- Labarriere N, Fortun A, Bellec A, Khammari A, Dreno B, Saiagh S, Lang F. A full GMP process to select and amplify epitope-specific T lymphocytes for adoptive immunotherapy of metastatic melanoma. *Clin Dev Immunol* 2013; 2013:932318; PMID:24194775; <http://dx.doi.org/10.1155/2013/932318>
- Kawakami Y, Eliyahu S, Delgado CH, Robbins PF, Rivoltini L, Topalian SL, Miki T, Rosenberg SA. Cloning of the gene coding for a shared human melanoma antigen recognized by autologous T cells infiltrating into tumor. *Proc Natl Acad Sci U S A* 1994; 91:3515-9; PMID:8170938; <http://dx.doi.org/10.1073/pnas.91.9.3515>
- Godet Y, Moreau-Aubry A, Guilloux Y, Vignard V, Khammari A, Dreno B, Jotereau F, Labarriere N. MELOE-1 is a new antigen overexpressed in melanomas and involved in adoptive T cell transfer

- efficiency. *J Exp Med* 2008; 205:2673-82; PMID:18936238; <http://dx.doi.org/10.1084/jem.20081356>
21. Youngblood B, Noto A, Porichis F, Akondy RS, Ndhlovu ZM, Austin JW, Bordi R, Procopio FA, Miura T, Allen TM et al. Cutting edge: Prolonged exposure to HIV reinforces a poised epigenetic program for PD-1 expression in virus-specific CD8 T cells. *J Immunol* 2013; 191:540-4; PMID:23772031; <http://dx.doi.org/10.4049/jimmunol.1203161>
  22. Youngblood B, Oestreich KJ, Ha SJ, Duraiswamy J, Akondy RS, West EE, Wei Z, Lu P, Austin JW, Riley JL et al. Chronic virus infection enforces demethylation of the locus that encodes PD-1 in antigen-specific CD8(+) T cells. *Immunity* 2011; 35:400-12; PMID:21943489; <http://dx.doi.org/10.1016/j.immuni.2011.06.015>
  23. Bouquie R, Bonnin A, Bernardeau K, Khammari A, Dreno B, Jotereau F, Labarrière N, Lang F. A fast and efficient HLA multimer-based sorting procedure that induces little apoptosis to isolate clinical grade human tumor specific T lymphocytes. *Cancer Immunol Immunother* 2009; 58:553-66; PMID:18751701; <http://dx.doi.org/10.1007/s00262-008-0578-2>
  24. Trautmann L, Labarrière N, Jotereau F, Karanikas V, Gervois N, Connerotte T, Coulie P, Bonneville M. Dominant TCR V alpha usage by virus and tumor-reactive T cells with wide affinity ranges for their specific antigens. *Eur J Immunol* 2002; 32:3181-90; PMID:12555663; [http://dx.doi.org/10.1002/1521-4141\(200211\)32:11%3c3181::AID-IMMU3181%3e3.0.CO;2-2](http://dx.doi.org/10.1002/1521-4141(200211)32:11%3c3181::AID-IMMU3181%3e3.0.CO;2-2)
  25. Orskov AD, Treppendahl MB, Skovbo A, Holm MS, Friis LS, Hokland M, Grønbaek K. Hypomethylation and up-regulation of PD-1 in T cells by azacytidine in MDS/AML patients: A rationale for combined targeting of PD-1 and DNA methylation. *Oncotarget* 2015; 6:9612-26; PMID:25823822; <http://dx.doi.org/10.18632/oncotarget.3324>
  26. Martinez GJ, Pereira RM, Aijo T, Kim EY, Marangoni F, Pipkin ME, Togher S, Heissmeyer V, Zhang YC, Crotty S et al. The Transcription Factor NFAT Promotes Exhaustion of Activated CD8 T Cells. *Immunity* 2015; 42:265-78; PMID:25680272; <http://dx.doi.org/10.1016/j.immuni.2015.01.006>
  27. Oestreich KJ, Yoon H, Ahmed R, Boss JM. NFATc1 regulates PD-1 expression upon T cell activation. *J Immunol* 2008; 181:4832-9; PMID:18802087; <http://dx.doi.org/10.4049/jimmunol.181.7.4832>
  28. Odorizzi PM, Pauken KE, Paley MA, Sharpe A, Wherry EJ. Genetic absence of PD-1 promotes accumulation of terminally differentiated exhausted CD8+ T cells. *J Exp Med* 2015; 212:1125-37; PMID:26034050; <http://dx.doi.org/10.1084/jem.20142237>
  29. Blank C, Brown I, Marks R, Nishimura H, Honjo T, Gajewski TF. Absence of programmed death receptor 1 alters thymic development and enhances generation of CD4/CD8 double-negative TCR-transgenic T cells. *J Immunol* 2003; 171:4574-81; PMID:14568931; <http://dx.doi.org/10.4049/jimmunol.171.9.4574>
  30. Nishimura H, Honjo T, Minato N. Facilitation of beta selection and modification of positive selection in the thymus of PD-1-deficient mice. *J Exp Med* 2000; 191:891-8; PMID:10704469; <http://dx.doi.org/10.1084/jem.191.5.891>
  31. Wong RM, Scotland RR, Lau RL, Wang C, Korman AJ, Kast WM, Weber JS. Programmed death-1 blockade enhances expansion and functional capacity of human melanoma antigen-specific CTLs. *Int Immunol* 2007; 19:1223-34; PMID:17898045; <http://dx.doi.org/10.1093/intimm/dxm091>
  32. Inozume T, Hanada K, Wang QJ, Ahmadzadeh M, Wunderlich JR, Rosenberg SA, Yang JC. Selection of CD8+PD-1+ lymphocytes in fresh human melanomas enriches for tumor-reactive T cells. *J Immunother* 2010; 33:956-64; PMID:20948441; <http://dx.doi.org/10.1097/CJI.0b013e3181fad2b0>
  33. Gervois N, Labarrière N, Le Guiner S, Pandolfino MC, Fonteneau JF, Guilloux Y, Diez E, Dreno B, Jotereau F. High avidity melanoma-reactive cytotoxic T lymphocytes are efficiently induced from peripheral blood lymphocytes on stimulation by peptide-pulsed melanoma cells. *Clin Cancer Res* 2000; 6:1459-67; PMID:10778978